

Manganese superoxide dismutase can reduce cellular damage mediated by oxygen radicals in transgenic plants

Chris Bowler¹, Luit Slooten²,
Saskia Vandenbranden², Riet De Rycke,
Johan Botterman³, Chris Sybesma²,
Marc Van Montagu and Dirk Inzé

Laboratorium voor Genetica, Rijksuniversiteit Gent, B-9000 Gent.
²Laboratorium voor Biofysica, Vrije Universiteit Brussel, B-1050
Brussel and ³Plant Genetic Systems N.V., Plateaustraat 22, B-9000
Gent, Belgium

¹Present address: Laboratory of Plant Molecular Biology, The
Rockefeller University, New York, NY 10021-6399, USA

Communicated by M. Van Montagu

In plants, environmental adversity often leads to the formation of highly reactive oxygen radicals. Since resistance to such conditions may be correlated with the activity of enzymes involved in oxygen detoxification, we have generated transgenic tobacco plants which express elevated levels of manganese superoxide dismutase (MnSOD) within their chloroplasts or mitochondria. Leaf discs of these plants have been analyzed in conditions in which oxidative stress was generated preferentially within one or the other organelle. It was found that high level overproduction of MnSOD in the corresponding sub-cellular location could significantly reduce the amount of cellular damage which would normally occur. In contrast, small increases in MnSOD activity were deleterious under some conditions. A generally applicable model correlating the consequences of SOD with the magnitude of its expression is presented.

Key words: *Nicotiana tabacum*/oxidative stress/paraquat/protein targeting/transgenic plants

Introduction

Reduced oxygen species such as superoxide radicals (O_2^-), hydrogen peroxide and hydroxyl radicals ($OH\cdot$) have been the subject of much research in recent years [for review, see Cadenas (1989)]. This interest has arisen because of the potential harm they can cause to all organisms exposed to an aerobic environment. Although neither O_2^- nor H_2O_2 at physiological concentrations seem particularly harmful, their toxicity *in vivo* arises by a metal ion-dependent conversion into hydroxyl radicals (the Haber–Weiss reaction), one of the most reactive species known to chemistry (Halliwell, 1987; Imlay and Linn, 1988). Of particular importance is its ability to mutate DNA and to initiate chain reactions of lipid peroxidation.

Oxy-radicals are by-products of many biological oxidations. For example, the electron transport chain of mitochondria is a well documented source of reactive oxygen species (Freeman and Crapo, 1982; Forman and Boveris, 1982; Ksenzenko *et al.*, 1983) whilst the oxygen-evolving functions within plant chloroplasts also make them particu-

larly susceptible to oxy-radical formation; electrons passing through the photosystems can react with oxygen to form superoxide radicals and hydrogen peroxide by a mechanism known as the Mehler reaction (Mehler, 1951; Asada and Takahashi, 1987).

In addition to their generation from these indigenous reactions, oxy-radical formation appears to be greatly increased during stress conditions. In animals, the role played by reduced oxygen species in ischemia/reperfusion injury, in some aspects of the aging process, in the development of inflammatory diseases such as rheumatoid arthritis and in the cytotoxicity of tumor necrosis factor (TNF) has been well documented (for reviews, see Bannister *et al.*, 1987; Jones, 1986; Halliwell, 1987). In plants, damage arising from environmental stresses often appears to be caused by oxy-radicals. For example, increased oxygen toxicity can be caused by air pollutants such as ozone and sulfur dioxide (Menzel, 1976; Chia *et al.*, 1984), certain herbicides (Harbour and Bolton, 1975; Orr and Hogan, 1983), chilling (Clare *et al.*, 1984), and high light intensities (Krause, 1988).

Organisms have evolved a wide range of enzymic and non-enzymic mechanisms to contend with this problem. Since hydroxyl radicals themselves are too reactive to be easily controlled, these mechanisms are designed to ensure that superoxide and hydrogen peroxide do not come into contact with each other. Of importance in this defense are anti-oxidants such as urate, glutathione, ascorbate and α -tocopherol, catalase and peroxidase enzymes which remove H_2O_2 , and superoxide dismutase (SOD) which converts superoxide to hydrogen peroxide. In many cases it appears that SOD is a key enzyme for providing protection against oxidative stress. Three forms of this enzyme exist, as classified by their metal cofactor: copper/zinc, manganese, and iron forms. The iron enzyme (FeSOD) is present in prokaryotes and within the chloroplasts of some plants. The manganese SOD (MnSOD) is widely distributed among prokaryotic and eukaryotic organisms and in eukaryotes it is most often found in the mitochondrial matrix. The copper/zinc enzyme (Cu/ZnSOD), however, is found almost exclusively in eukaryotic species where it is normally present in the cytosol and in addition some plants contain a chloroplastic isoform (for review, see Bannister *et al.*, 1987).

The importance of SOD for aerobic growth has been demonstrated in several ways. SOD-deficient mutants of *Escherichia coli* (Carlioz and Touati, 1986) and yeast (Biliński *et al.*, 1985; van Loon *et al.*, 1986) are hypersensitive to oxygen, and a null mutation of Cu/ZnSOD in *Drosophila* results in infertility and a reduction of life span (Phillips *et al.*, 1989). Over-production of manganese superoxide dismutase in human cells partially protects cells against the cytotoxicity of tumor necrosis factor (TNF) (Wong *et al.*, 1989). In plants, resistance to air pollutants such as ozone and SO_2 has been shown to correlate with increased levels of enzymes involved in superoxide detoxification in poplar and in *Phaseolus vulgaris* (Tanaka

and Sugahara, 1980; Lee and Bennett, 1982). Increased resistance to photo-oxidative damage in ripening tomato fruits is correlated with SOD (Rabinowitch *et al.*, 1982) and the presence of the enzyme in rhizomes of *Iris* under anaerobic conditions has been found to be important for their ability to recover from anoxic stress (Monk *et al.*, 1987).

However, some data suggest that SOD activity is not the limiting factor determining cell survival under adverse conditions. Transgenic plants which contain high levels of Cu/ZnSOD within their chloroplasts appear to be no more resistant to superoxide toxicity than normal plants (Tepperman and Dunsmuir, 1990). Moreover, in specific cases SOD has also been shown to cause detrimental effects. For example increased activity of cytosolic Cu/ZnSOD arising from a trisomy of chromosome 21 in Down's syndrome (DS) patients may be a causative agent of some of the disease symptoms. Low-level overproduction of cytosolic Cu/ZnSOD in rat cells results in impaired neurotransmitter uptake (Elroy-Stein and Groner, 1988) and transgenic mice which overproduce the enzyme develop abnormalities within the tongue neuromuscular junctions similar to those observed in tongue muscle of patients with DS (Avraham *et al.*, 1988).

If nothing else, these contradictory results demonstrate that some cell types are affected by perturbations in SOD activity levels, although the reasons why this is so have not been elucidated. In an attempt to clarify some of the questions raised by these results and also to evaluate the potential capabilities of SOD for plant stress tolerance, we have engineered plants which overproduce a MnSOD specifically within their mitochondria or chloroplasts. Utilizing model systems which generate an oxidative stress preferentially within each of these compartments, we demonstrate here that organellar MnSOD can provide protection against superoxide-mediated damage within these subcellular environments, although under some conditions it can also be deleterious. We believe that the determining factor is the ratio between superoxide and hydrogen peroxide within the cell. In addition to being the SOD substrate and reaction product, these are the two Haber-Weiss reaction substrates from which hydroxyl radicals can be generated. The implications of these results for further understanding the general importance of SOD to the survival of multicellular organisms and specifically for the engineering of plants more tolerant to environmental adversity are discussed.

Results

Generation of plants which produce elevated levels of MnSOD

In *Nicotiana plumbaginifolia*, MnSOD is a nuclear-encoded protein which is targeted to the mitochondria. The isolation of a full-length cDNA encoding this protein has been previously described (Bowler *et al.*, 1989a) and studies in yeast have shown that the mitochondrial targeting is mediated by an N-terminal leader sequence (Bowler *et al.*, 1989b). To make a construction which would overproduce MnSOD in the mitochondria of plants, we inserted the entire coding sequence downstream of the CaMV 35S promoter of binary vector pGSJ780A (see Materials and methods), generating plasmid pMitSOD (Figure 1a). Similarly, for targeting MnSOD to chloroplasts, we first replaced the mitochondrial leader sequence with a transit peptide for chloroplast

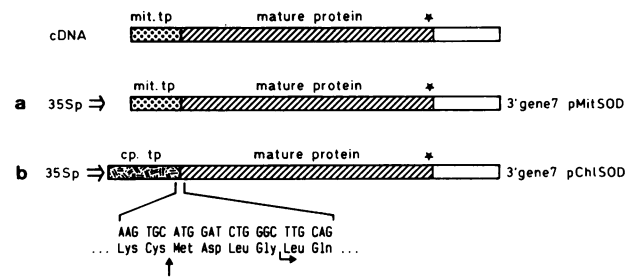


Fig. 1. Schematic representation of constructions for mitochondrial and chloroplastic targeting of MnSOD. The mitochondrial leader sequence-encoding DNA (mit.tp) is denoted by a dotted box, the mature protein-encoding sequence as a hatched box (with an asterisk representing the stop codon) and the sequence encoding the chloroplast transit peptide (cp.tp) as a striated box. Each cassette is flanked at the 5' end by the 35S promoter (35Sp) and at the 3' end by polyadenylation signals of the T-DNA-encoded gene 7 (3' gene 7). The sequence and corresponding amino acids at the fusion of the chloroplast transit peptide and MnSOD mature protein in pChlSOD (b) are shown. The predicted processing site is indicated by a vertical arrow and the normal NH₂-terminus of the MnSOD mature protein is shown by a horizontal arrow. For details of the constructions, see Materials and methods.

targeting and then placed this cassette downstream of the 35S promoter. This construct was designated pChlSOD (Figure 1b).

These constructions were subsequently introduced into *Nicotiana tabacum* cv. PBD6 by conventional leaf disc transformation (De Block *et al.*, 1987). Total soluble proteins were extracted from leaves of individual transgenic plants (15 plants for each construction) and were first assayed for MnSOD activity on native polyacrylamide gels. Most of the putative transformants were found to contain a new MnSOD activity (data not shown) and based on this analysis, for each construction, two plants which contained the highest levels were selected for further study. These were designated MitSOD1 and MitSOD2 for the mitochondrial targeting construct, and ChlSOD1 and ChlSOD2 for the chloroplast targeting construct. It should be noted that we also designed a construct to produce MnSOD in the cytosol of plants. Although the protein product was active and transcript abundance was equivalent to that in MitSOD and ChlSOD plants, protein levels were extremely low, apparently a result of protein instability (data not shown). Consequently these plants were not studied further.

To determine whether the MnSOD was targeted to the correct subcellular location, we prepared mitochondria and chloroplasts from mature leaves of MitSOD1 and ChlSOD1 transformants. Figure 2 details the results of this analysis. Untransformed *N. tabacum* appears to contain five electrophoretically distinguishable SOD enzymes: three Cu/ZnSODs, one MnSOD and one FeSOD (Figure 2a). The MnSOD co-purifies with mitochondrial fractions and the FeSOD is present within highly purified chloroplasts. A similar situation exists in the related *N. plumbaginifolia* (Van Camp *et al.*, 1990) from which the MnSOD cDNA was derived. However, the *N. plumbaginifolia* MnSOD migrates faster than the *N. tabacum* MnSOD (e.g. Figure 2b), which allows the engineered SOD to be distinguished from the endogenous enzyme in the transgenic plants.

The activity of the new MnSOD in MitSOD1 and ChlSOD1 plants adds significantly to the endogenous activities (Figure 2b and c). The additional MnSOD activity

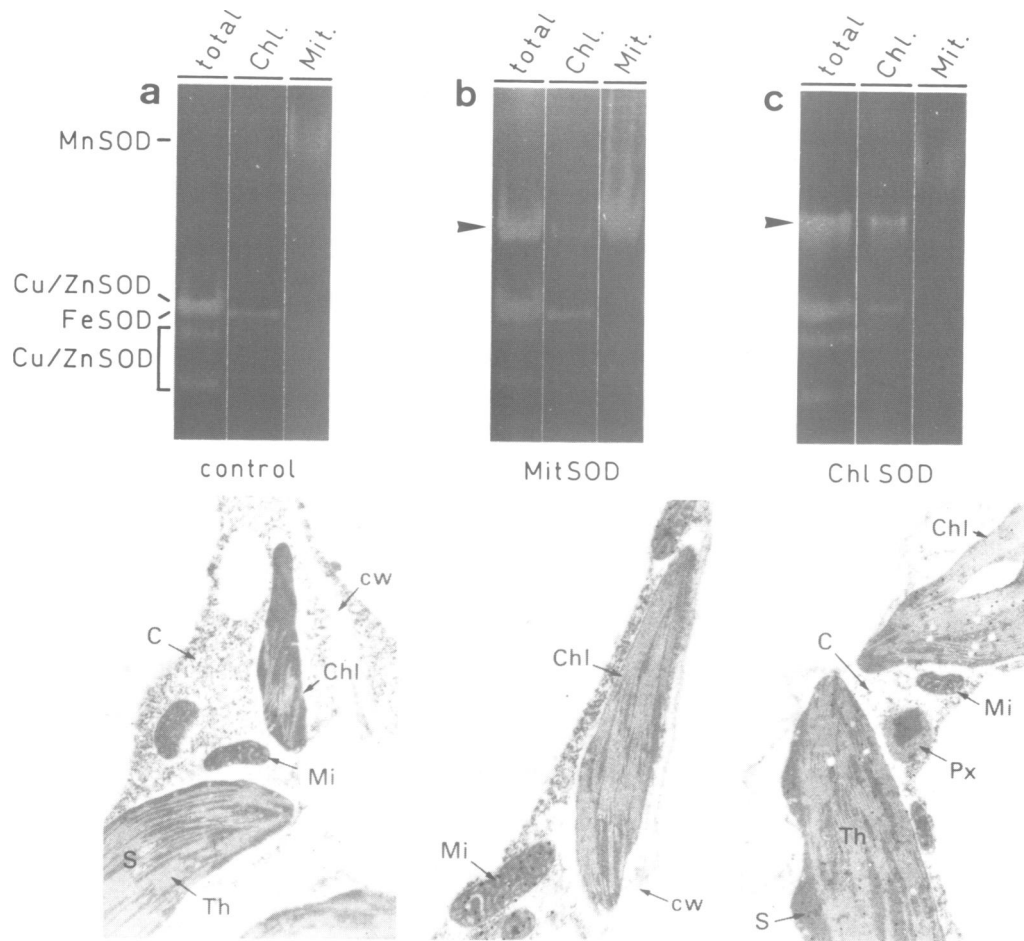


Fig. 2. Targeting of engineered MnSOD to mitochondria and chloroplasts of MitSOD1 and ChlSOD1 plants, respectively, revealed by subcellular fractionations (upper panel) and immunogold labelling of electron micrograph sections (lower panel). (a) SOD protein profile on native polyacrylamide gels of untransformed tobacco (cv. PBD6). The three cytosolic Cu/ZnSODs, the chloroplastic FeSOD and the mitochondrial MnSOD are indicated. The three types of SOD were identified using inhibitor studies (Van Camp *et al.*, 1990). (b) SOD profile of MitSOD1 plants. (c) SOD profile of ChlSOD1 plants. The overproduced MnSOD is indicated in each case with an arrow. Abbreviations: total, 100 μ g total soluble proteins; Chl., 50 μ g protein extracted from Percoll-purified chloroplasts; Mit., 50 μ g protein from Percoll-purified mitochondria. The lower panel shows representative immunogold labellings of sections derived from these plants. Abbreviations: C, cytosol; Chl, chloroplast; cw, cell wall; Mi, mitochondria; Px, peroxisome; S, stroma; Th, thylakoid membrane.

in MitSOD1 co-purifies predominantly with mitochondrial fractions, although some activity is present in the chloroplast fractions (Figure 2b). We presume this to be a result of mitochondrial contamination in the samples. In contrast to MitSOD1, the new MnSOD activity in ChlSOD1 co-purifies exclusively with the endogenous FeSOD in chloroplast fractions (Figure 2c), demonstrating that the enzyme can be targeted to, and retain its activity in, a foreign location.

Information obtained from the subcellular fractionations was confirmed by immunogold labelling of sections derived from untransformed and transgenic plants with polyclonal antibodies raised against *N.plumbaginifolia* MnSOD (Figure 2). Although expression of the endogenous MnSOD was too low to be detected, the electron micrographs clearly show labelling specifically within mitochondria of MitSOD1 plants (Figure 2b) and chloroplasts of ChlSOD1 plants (Figure 2c). We found no evidence for anomalous targeting to other locations in any sections examined. Based on both enzymatic activity and immuno-reactivity, the engineered MnSOD in MitSOD2 and ChlSOD2 plants was identical to that in MitSOD1 and ChlSOD1 plants, respectively (data not shown).

Properties of chimeric MnSOD gene expression in transgenic plants

Although transgenic plants which overproduce MnSOD in either chloroplasts or mitochondria show no apparent peculiarities during development, it was of great interest to examine the effects of organellar SOD overproduction at the cellular level, particularly during conditions which generate oxidative stress. For these experiments, detailed in the following sections, we chose to use assays which employed leaf discs derived from leaves at different developmental stages. Three types of leaves were studied: 'rosette leaves' from young plants (6–9 weeks old), and immature and mature (i.e. fully expanded) leaves from older bolting plants (> 13 weeks old and with stems longer than 45 cm). These are denoted, respectively, as 'young bolting' and 'old bolting' leaves. The young bolting leaves have approximately half the length and width of old bolting leaves.

Before assessing the consequences of increased SOD activity, it was necessary to determine the level of augmentation in these different leaf types. The results of this analysis are shown in Figure 3. When SOD activity is assayed in all the leaves down the stem of bolting plants,

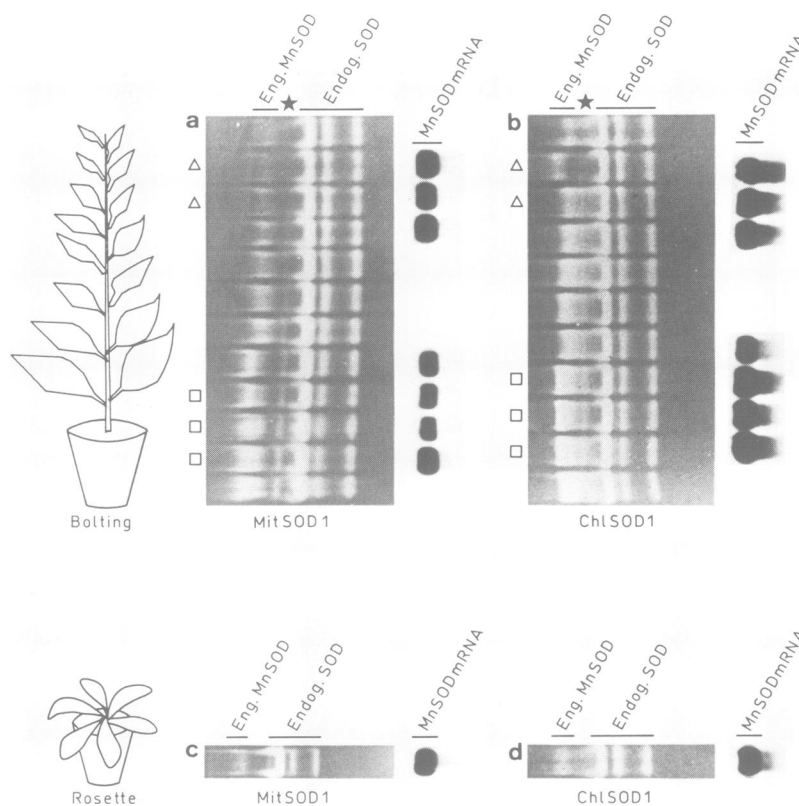


Fig. 3. MnSOD mRNA and SOD activity profiles in different leaves of MitSOD1 and ChlSOD1 plants. Total RNA and total soluble proteins were isolated from leaves down the stem of bolting plants and from rosette plants (see diagrams) and analyzed for steady-state MnSOD mRNA and for SOD activity. **Panels a** and **c** show the results from a MitSOD1 plant and **panels b** and **d** show the data obtained from a ChlSOD1 plant. The engineered (eng. MnSOD) and endogenous SOD (endog. SOD) activities are indicated. The asterisk shows the position of the endogenous 'senescence-related' MnSOD. The symbol Δ indicates the type of leaves referred to in the text as 'young bolting', and \square denotes 'old bolting'-type leaves. Each sample loaded on the protein gels contains 80 μ g total soluble protein. MitSOD2 and ChlSOD2 plants show very similar profiles to those given here (data not shown). The abundance of MnSOD mRNA in different leaf types is also shown in each panel. Transcript levels are always slightly higher in both ChlSOD plants than in the MitSOD plants. Since the number of copies of the introduced gene has not been assessed this may, however, be a result of copy number rather than of a particular effect at the level of transcription.

it can be seen that the endogenous SOD activity does not change significantly (Figures 3a and b). However, activity of the enzyme synthesized from the chimeric MnSOD genes increases dramatically with age in both MitSOD and ChlSOD plants. The endogenous MnSOD is too low to be detected in the amounts of protein loaded on these gels but by making a dilution series of extracts, we estimate that the increase in MnSOD activity in mitochondria of old bolting leaves is ~30-fold in MitSOD plants. Young bolting leaves from MitSOD plants only have a 3-fold increase in MnSOD activity. Similarly, the levels of MnSOD activity in the chloroplasts of old and young bolting leaves of ChlSOD plants were estimated to be 50-fold and 10-fold higher, respectively, when compared with the endogenous MnSOD activity present in the mitochondria of these plants. However, the total chloroplastic SOD activities (made up of the combined activities of engineered MnSOD and the endogenous FeSOD) are only augmented 3-fold and 0.6-fold in old and young bolting leaves of ChlSOD plants, respectively. The levels of elevated SOD activity in leaves at the rosette stage from both MitSOD and ChlSOD plants are the same as for young bolting leaves. The two MitSOD plants did not differ significantly from each other with respect to SOD activity levels, nor did the two ChlSOD plants (data not shown). Also visible on such gels is an additional band of SOD activity only present in older leaves (indicated by

an asterisk in Figure 3a and b), migrating slightly faster than the introduced MnSOD enzyme. This activity is also present in untransformed plants (data not shown) and our data suggests that it is a MnSOD. This 'senescence-related' activity has hitherto been unreported.

In spite of this dramatic gradient of chimeric MnSOD activity down the stem, the levels of steady-state mRNA are equivalent in all leaves of MitSOD and ChlSOD plants (Figure 3a–d), indicating that this phenomenon is a post-transcriptional event.

Chloroplastic MnSOD provides resistance against oxidative stress generated within the chloroplasts

To study the cellular effects of SOD over-production we have developed model systems based on the use of methyl viologen (MV), a herbicide also known as paraquat. It is well known that during illumination, MV preferentially accepts electrons from photosystem I and donates them to oxygen, thus forming the superoxide radical within the chloroplasts (reviewed in Halliwell, 1984). The development of the methods to assess the amount of cellular damage arising from such treatments will be documented in detail in a separate article (Slooten, L., Bowler, C., Vandenbranden, S., Van Montagu, M., Inzé, D. and Sybesma, C., in preparation). Essentially, rectangular leaf discs of equal size cut from equivalent leaves of untransformed control,

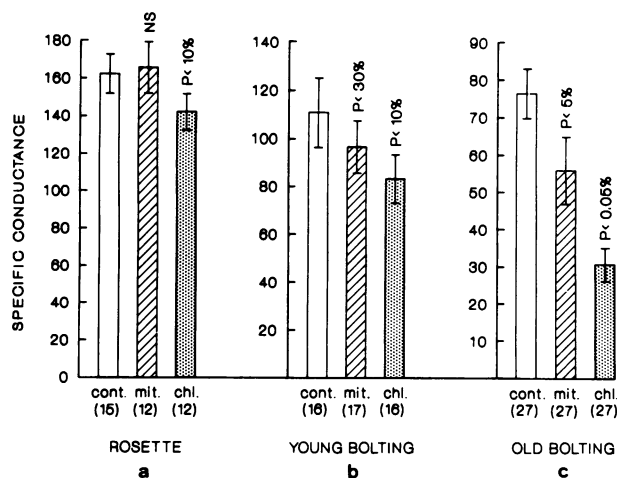


Fig. 4. Light-dependent MV-induced increases in specific conductance expressed as the values $\times 10^6 \times \Omega^{-1} \text{ cm}^{-1}$ per 35 mg fresh weight. The values given show the mean \pm standard error of the mean for control (cont.), MitSOD (mit.) and ChlSOD (chl.) material at the rosette (a), young bolting (b) and old bolting (c) stages. The vertical scale is slightly different for each panel, reflecting the differing sensitivity of young and old material to MV. The MV concentrations were $0.5 \mu\text{M}$ (a) and $1.2 \mu\text{M}$ (b and c), and the other experimental conditions are as outlined in Materials and methods. The number of leaf discs from which these values were calculated is shown underneath each bar. NS indicates no significant difference in comparison with control plants. P denotes the probability that the results are not significantly different from those obtained with control plants. These probabilities were calculated using Welch's modification of Student's t-test, applicable to populations with unknown variances (Welch, 1947). The specific conductance of the floating solutions of leaf discs without MV was on the order of $16 \times 10^{-6} \Omega^{-1} \text{ cm}^{-1}$ per 35 mg fresh weight. The open boxes represent control plants; the hatched boxes MitSOD plants, and the stippled boxes ChlSOD plants.

MitSOD and ChlSOD plants were floated on solutions of MV in Petri dishes and illuminated as described in Materials and methods. As mentioned in the previous section, we tested rosette, old bolting and young bolting leaves.

Cellular injury within these leaf discs was assessed firstly by measuring the conductance of the floating solution. This measures the leakage of ionic solutes out of the cells and hence gives an indication of membrane damage. Lipid peroxidation resulting from oxidative stress is likely to initiate this membrane deterioration. Light-dependent MV damage as measured by conductance is shown for a typical series of plants in Figure 4. This figure summarizes data from six control plants and two plants each of MitSOD1 and MitSOD2 (grouped as MitSOD), and ChlSOD1 and ChlSOD2 (collectively ChlSOD). The different control plants did not differ significantly from each other in this assay, likewise the four MitSOD plants and the four ChlSOD plants. These plants did not show any differences in their 'background' level of conductance (i.e. from leaf discs floated on water alone) revealing that membrane integrity was not altered by changes in SOD activity *per se*.

Rosette leaves and young bolting leaves, each having comparatively low SOD overproduction, show only slight differences with respect to each other (Figure 4a and b): MitSOD material behaves very similarly to control leaves, whereas ChlSOD leaves show slightly less damage (significant at 90% probability). However, in old bolting leaves, where MnSOD activity is maximal, the differences become much more pronounced (Figure 4c). Leaves from MitSOD plants are slightly protected against light-dependent MV damage (significant to 95%) and the resistance of ChlSOD

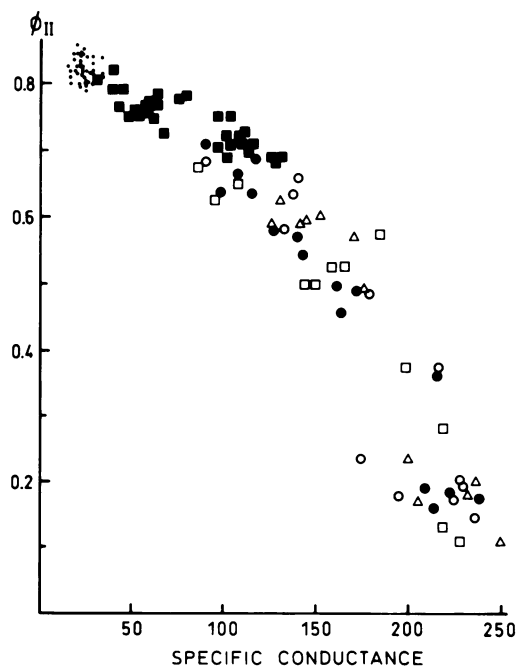


Fig. 5. Scattergram of Φ_{II} and specific conductance data from leaf discs for which both parameters were measured. Specific conductance is expressed as in Figure 4. Symbols: \circ , \bullet control (rosette and old bolting, respectively); \triangle , \blacktriangle MitSOD (rosette and old bolting, respectively). Small dots indicate the values obtained from leaf discs of all types of plants not treated with MV. The Φ_{II} values were determined as described in Materials and methods.

material is now highly significant at 99.95% probability. These leaves show ~ 2.5 -fold less damage than the controls. These data imply that the degree of damage is negatively correlated with the level of MnSOD overproduction. The observation that the effects of ChlSOD overproduction are much more pronounced than equivalent levels of MitSOD overproduction is consistent with the fact that the formation of superoxide radicals is being biased to the chloroplasts in light conditions.

To examine chloroplast-localized effects, we used chlorophyll fluorescence techniques to determine the integrity of various components of the photosynthetic apparatus (for review, see Krause and Weis, 1984). Several parameters were studied (Slooten, L., Bowler, C., Vandenbranden, S., Van Montagu, M., Inzé, D. and Sybesma, C., in preparation) and one example, Φ_{II} , the quantum yield of exciton trapping by the reaction center of photosystem II, will be documented here. This parameter essentially gives a measure of the integrity of the photosystem II reaction center. In some experiments, after incubation in MV, the fluorescence properties of the leaf discs were analyzed and Φ_{II} values determined. Hence, for these experiments we have a value for conductance and for Φ_{II} . When the data from these are plotted in a scatter diagram (Figure 5), it is clear that these two parameters are correlated, i.e. as photosystem II becomes progressively damaged (low Φ_{II} values), cell membrane damage also increases (high conductance).

Another important conclusion from this analysis is that the data from all types of leaves from control, MitSOD and ChlSOD plants are scattered randomly along the line, except for the values from old bolting ChlSOD leaves. These values are uniformly grouped together at the upper left end of the plot, the position corresponding to minimal cellular damage. Hence high level MnSOD overproduction in the chloroplasts

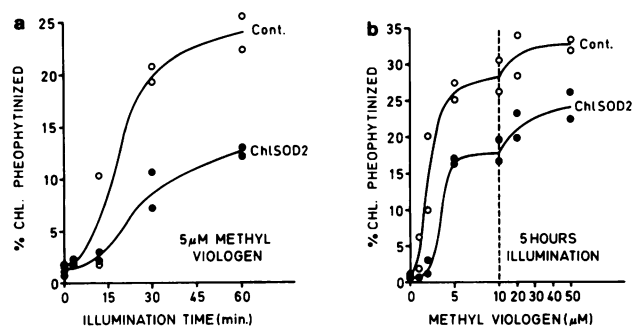


Fig. 6. Light-dependent MV-induced increases in pheophytin in leaf discs derived from old bolting control (○) and ChlSOD2 (●) leaves. (a) Percentage of chlorophyll pheophytinized as a function of illumination time in the presence of 5 μM MV. Experimental conditions were exactly as described in Materials and methods, except for these alterations in illumination time. (b) Pheophytin appearance induced by increasing concentrations of MV with 5 h of illumination. The dashed vertical line distinguishes between the two scales used on the horizontal axis.

can protect both the photosynthetic apparatus and the cellular membranes from MV-generated damage in this model system.

Furthermore, we have examined the effects of oxygen radical stress on the pigment content of leaves. One of the consequences of the light incubations in the presence of MV is that in the subsequent dark period, chlorophyll is pheophytinized, i.e. it loses its central magnesium atom. It has been shown recently that free fatty acids destabilize the chloroplastic pigment-protein complexes, rendering the chlorophyll susceptible to pheophytinization (Siefermann-Harms, 1990). We assume that lipid peroxidation resulting from oxidant damage to membranes is mediating this destabilization and consequent pheophytin formation.

Figure 6 shows a representative example of pheophytin formation in leaf discs derived from old bolting leaves of control and ChlSOD plants as a function of illumination time (Figure 6a) and MV concentration (Figure 6b). In both cases less pheophytin is formed in the ChlSOD material than in the untransformed leaf material.

In summary, we have shown that in this model system, where MV damage is light-dependent, high level overproduction of MnSOD in the chloroplasts can significantly reduce the normal level of oxidative damage, protecting both the compartment where free radicals were generated and the cellular membranes as well. The experiments described above have been repeated with three sets of plants and in all cases the results are comparable to those documented here (data not shown).

Effects of MnSOD on the damage generated by methyl viologen in the dark

Although the light-mediated MV toxicity is primarily a consequence of electrons being donated to MV from photosystem I, MV may also be accepting some electrons from a mitochondrial source, most likely the respiratory electron transport chain, and hence forming the superoxide anion within this organelle. By incubating leaf discs with MV in the dark, it may be possible to analyze the effects of superoxide formation in the mitochondria since photosynthetic electron transport will be inoperative. Indeed, when leaf discs are incubated with MV in the dark in the presence of inhibitors of mitochondrial electron transport, the resulting

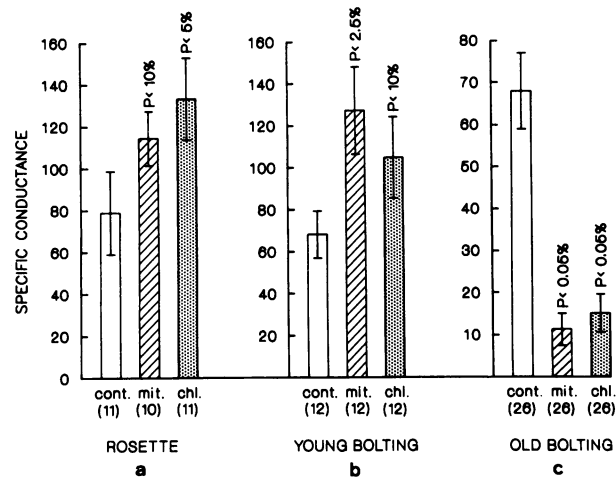


Fig. 7. MV-induced increases in specific conductance in dark experiments. All parameters are denoted as in Figure 4. The MV concentrations were 0.5 μM (a) and 1.2 μM (b and c).

damage is reduced by $\sim 30\%$, whereas no reduction was observed in the light (Slooten, L., Bowler, C., Vandenbranden, S., Van Montagu, M., Inzé, D., and Sybesma, C., in preparation).

Having developed a reproducible model system for carrying out such dark incubations (see Materials and methods) we then examined the damage generated in control, MitSOD and ChlSOD material. Using the same plants as were studied in the light experiments, rosette, young bolting and old bolting leaves were again examined using conductance as a measure for cellular damage. The results in Figure 7 show clearly that different effects are observed in the dark than were previously seen in the presence of light (compare with Figure 4). Material in which MnSOD is only moderately overproduced, either in chloroplasts or mitochondria (i.e. rosette and young bolting leaves) is actually more sensitive to MV than control material (Figure 7a and b), indicating that low levels of MnSOD overproduction are detrimental for the cells during these dark incubations. However in old bolting leaves displaying maximal MnSOD activity the effects are reversed: both mitochondrial and chloroplastic MnSOD now provide high level protection (Figure 7c) significant at the 99.95% probability levels. These results imply that the level of MnSOD overproduction plays a critical role in determining the effects which follow in this model system. Additionally, since chloroplastic MnSOD has a similar influence to the mitochondrial MnSOD, it would appear that superoxide is still present within the chloroplasts in dark conditions. For each leaf disc, fluorescence measurements were also made, again revealing a direct correlation between $\Phi\Pi$ values and conductance values (data not shown). Once more the conclusion is that whilst O_2^- generation may be confined to specific cell locations under different physiological conditions, the damage that is produced pervades the entire cell.

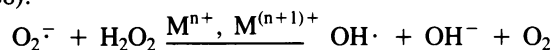
Discussion

The potential use of SOD for the genetic engineering of plant stress resistance has been often suggested but never thoroughly investigated. In this study we have chosen to evaluate the properties of MnSOD overproduction in plant mitochondria and chloroplasts. MnSOD was chosen rather

than Cu/ZnSOD or FeSOD because it is not inactivated by the reaction product H_2O_2 , as are the other two enzymes. Consequently any effects observed can be thought of simply as a result of a change in the ratio between the SOD substrate and product (i.e. O_2^- and H_2O_2), this change being directly proportional to the level of SOD augmentation and being unaffected by H_2O_2 concentration.

The effects of MnSOD overproduction were analyzed on leaf discs using MV as a superoxide radical-generating agent. This reproducible model system to study the effects of oxygen radical formation at the cellular level has several advantages over the use of whole plants. First, it is easier to quantify the amount of MV applied to a leaf disc than it is to quantify that applied to an intact leaf or an intact plant. Experiments on whole plants show much variation and produce large statistical errors which can only be averaged out by using a much larger number of plants than can be handled in laboratory conditions. A second problem of MV application on whole plants is that the degree of damage caused by the compound is light dependent. Since all leaves will not receive the same amount of light, the observed MV damage will greatly vary.

We were able to test the effects of different levels of SOD overproduction because of the unexpected gradient of MnSOD activity which exists from young to old leaves of transgenic plants. Although its cause is not known, its experimental exploitation has revealed that the level of SOD overproduction can be instrumental in determining the amount of damage generated by the redox-active compound methyl viologen (MV). MV acts by accepting electrons and donating them to oxygen, thus forming the superoxide anion. Its effects have been studied in leaf discs incubated in light and dark conditions. The most surprising observation we made was that both positive and negative effects can arise, apparently dependent upon the level of SOD overproduction. To what extent do these results conform to the theories currently held of oxygen radical toxicity? Central to these ideas is a metal (M) ion-catalyzed Haber–Weiss reaction, involving the formation of highly reactive hydroxyl radicals ($\text{OH}\cdot$) from the comparatively unreactive superoxide anion and hydrogen peroxide (Halliwell, 1987; Imlay and Linn, 1988):



Hence, SOD would be likely to play an important role in cellular defense against oxidative stress since it has the unique property of controlling the ratio of O_2^- and H_2O_2 , the two Haber–Weiss reaction substrates. The remainder of this discussion will examine the support which our results give to these ideas and will attempt to explain other contradictions previously reported from both prokaryotic and eukaryotic systems.

In our light experiments, the superoxide anion is likely to be formed predominantly within the chloroplasts due to the high rate of electron transfer through the photosystems. In the absence of sufficient SOD, the presence of both O_2^- and H_2O_2 would ensure the formation of $\text{OH}\cdot$ which can then initiate destructive processes. The consequence of MnSOD over-production in the chloroplasts would be to reduce the levels of O_2^- and to increase the levels of H_2O_2 . The H_2O_2 can then be controlled by the H_2O_2 -scavenging pathway of chloroplasts, which has been shown to be active in the light but not in the dark (Foyer and Halliwell, 1976;

Nakano and Asada, 1980). SOD can thus act synergistically with this pathway to remove the Haber–Weiss reaction substrates, thereby reducing the damage generated by MV by amounts correlating with its level of overproduction.

In dark experiments this simple relationship between SOD activity levels and the extent of damage does not exist. It appears that low levels of chloroplastic MnSOD are detrimental, but above a certain level this effect is completely reversed. Since chloroplastic H_2O_2 -scavenging is not operational in the dark, it is conceivable that low level MnSOD overproduction merely serves to upset the normally optimized balance between O_2^- and H_2O_2 , thereby making the formation of $\text{OH}\cdot$ more likely and consequently increasing the damage. High level overproduction would shift the $\text{O}_2^-:\text{H}_2\text{O}_2$ equilibrium almost completely over to H_2O_2 , thus ensuring that little O_2^- is available for the Haber–Weiss reaction and resulting in a reduction in cellular damage. These effects were clearly observed (Figure 7).

Since the chloroplastic MnSOD shows such striking effects in our dark experiments, a significant proportion of superoxide must still be present in the chloroplast. It is possible that this is generated elsewhere and diffuses in, following its protonation ($\text{pK}_a = 4.7$), or that it is generated within the chloroplast. Isolated chloroplasts have been shown to reduce MV in the dark (Law *et al.*, 1983) suggesting that O_2^- could in fact be generated *in situ*. A chlororespiratory electron transport pathway is known to be stimulated in the dark in photosynthetic prokaryotes and green algae and recent evidence suggests that it is also present in plant chloroplasts (Garab *et al.*, 1989). This may then provide a chloroplastic source of electrons for MV in the dark.

The effects of increased mitochondrial MnSOD activity are not particularly pronounced in the light experiments presumably because the majority of superoxide is being generated within the chloroplasts. However when activity levels are high, even this spatially restricted enzyme appear to provide low levels of protection, perhaps destroying the superoxide formed within mitochondria or acting as a sink for superoxide diffusing in from the cytosol. In the dark, however, the effects are more pronounced and are essentially the same as observed for the chloroplastic MnSOD—low levels being detrimental whilst high levels are beneficial. Although almost nothing is known about H_2O_2 -scavenging within plant mitochondria, the results can again be explained by the perturbation of the normal $\text{O}_2^-:\text{H}_2\text{O}_2$ ratio, i.e. low MnSOD activity levels changing the equilibrium closer to 1:1, favoring $\text{OH}\cdot$ formation, and high MnSOD activity levels ensuring the presence of only low amounts of O_2^- and hence reduced $\text{OH}\cdot$ formation.

This model is fully consistent with the hypothesis that the Haber–Weiss reaction is the prime culprit for oxygen toxicity *in vivo*. It also incorporates the phenomenon of light-dependent H_2O_2 scavenging in chloroplasts and acknowledges the possible existence of chlororespiration in plants. Additionally both positive and negative effects of Cu/ZnSOD overproduction have been observed in human and mouse cells (Elroy-Stein *et al.*, 1986) and with MnSOD in *E. coli* (Bloch and Ausubel, 1986; Gruber *et al.*, 1990), in all cases the likely cause being the differences in the levels of SOD overproduction, i.e. the particular consequence is dependent on how SOD affects the ratio between O_2^- and H_2O_2 , either making $\text{OH}\cdot$ formation from the Haber–Weiss reaction more likely or less likely.

Nevertheless, other factors should be considered. Obvious differences between the above mentioned experiments are the type of SOD studied, either Cu/ZnSOD or MnSOD, and the subcellular location. It is prudent to remember that Cu/ZnSOD is inactivated by H_2O_2 whereas MnSOD is not. This may be the possible reason why small increases of Cu/ZnSOD can provide resistance against MV in human and mouse cells whereas higher levels cannot (Elroy-Stein *et al.*, 1986). As such, in high producing lines the burst of H_2O_2 generated by the combined action of MV and SOD may simply inactivate the Cu/ZnSOD, leading to the existence of both O_2^- and H_2O_2 within the cell, and hence hydroxyl radicals. This can also explain the discrepancy in the results obtained by Tepperman and Dunsmuir (1990) in comparison with ours. They analyzed the effects of high level overproduction of a Cu/ZnSOD in tobacco chloroplasts in systems analogous to ours and found neither positive nor negative effects with regard to light-dependent MV damage to plant cells. In the leaves examined, the level of overproduction appeared comparable to the high levels which we observed in older leaves, so again the lack of any effect may simply be due to the inactivation of the Cu/ZnSOD by H_2O_2 . Unfortunately, Cu/ZnSOD activity levels in the material before and after stress treatment was not examined in either case.

The subcellular location is also likely to play an important role in determining whether positive or negative effects arise from SOD overproduction. Furthermore, not only the amount of SOD present within the different cellular compartments, but also their endogenous H_2O_2 -scavenging abilities will influence the turnover and accumulation of reactive products as well as the continued activity of SOD under stress conditions. Therefore, it remains possible that the dependence of the observed effects on leaf age reflects differences not only in SOD activity levels but also in the physiological states of the different leaf types.

In summary, it is clear that SOD can be manipulated to give resistance to oxidative stress although there is clearly a fine line between benefit and injury, dependent upon the level of overproduction, the type of SOD used and the endogenous scavenging systems of the organism, with everything being ultimately dependent upon the $O_2^-:H_2O_2$ ratio. Our results support the use of MnSOD expressed at high levels as the most promising route of SOD for developing stress tolerance in plants. Also, since our model systems have revealed both mitochondrial and chloroplastic MnSOD to be beneficial, it is likely that a plant which contains elevated MnSOD in both organellar compartments will be even more resistant to MV. This awaits analysis, as does the effects of cytosolic MnSOD overproduction.

Finally it remains to be seen whether visible phenotypes will be observed at the whole plant level with regard to economically relevant stress conditions such as chilling, high light intensities and pollutants such as ozone. Plant varieties which are tolerant to MV (in the form of the herbicide paraquat) often show cross-tolerance to adverse environmental conditions, thus implicating the involvement of oxidative damage in many of these processes (e.g. Tanaka *et al.*, 1988; Shaaltiel *et al.*, 1988), and suggesting that the transgenic plants which we have generated may also show similar phenotypes. However, whether the degree of protection observed at the cellular level will be sufficient to provide such a resistant phenotype at the whole plant level

remains to be tested and it may prove necessary to supplement an engineered SOD enzyme with other oxygen-detoxifying enzymes such as catalase or peroxidase to produce a desirable phenotype.

Materials and methods

Construction of MnSOD expression cassettes

Expression cassettes were constructed in binary vectors pGSJ780A (derived from pGSFR780A; De Block *et al.*, 1989) and pGSC1702 (derived from pGSC1700; Cornelissen and Vandewiele, 1989). Between the T-DNA borders, each of these vectors contains the neomycin phosphotransferase II (*nptII*) gene under control of the nopaline synthase (*nos*) promoter (Depicker *et al.*, 1982) for kanamycin selection of transformed cells. In addition, pGSJ780A contains the cauliflower mosaic virus (CaMV) 35S promoter (from pGSJ280; Deblaere *et al.*, 1987) immediately upstream of unique *ClaI* and *BamHI* sites which can be used, respectively, to create transcriptional or translational fusions to foreign protein-coding sequences.

pMitSOD was constructed by inserting the entire coding sequence of the MnSOD cDNA as a 960 bp *HpaI*–*SmaI* fragment from pSOD1 (Bowler *et al.*, 1989a) into the blunt-ended, dephosphorylated *ClaI* site of pGSJ780A (Figure 1a). This generates a transcriptional fusion of the MnSOD to the 35S promoter.

To construct pChlSOD it was necessary to create a fusion between the MnSOD mature protein and a transit peptide for chloroplast targeting. This was done by cutting pSOD1 with *SacI*, which recognizes a unique site at the junction between the mitochondrial leader sequence-encoding DNA and the mature MnSOD-encoding sequence, flushing with T4 DNA polymerase and adding an octameric *BglII* linker to create plasmid pSODB. The mature protein-encoding sequence was then inserted as a *BglII*–*BamHI* fragment into the dephosphorylated *BamHI* site of pKAHI (J. Botterman, unpublished data). This *BamHI* site is immediately downstream of a sequence encoding the 35S promoter coupled to the sequence encoding the transit peptide of a small subunit gene of ribulose-1,5-bisphosphate carboxylase (SS_{Tp}) from pea (Cashmore, 1983). This generates an in-frame fusion of the chloroplast transit peptide with the MnSOD mature protein. Once processed the MnSOD will contain four additional N-terminal amino acids (Met-Asp-Leu-Gly) generated as a consequence of the cloning procedure (Figure 1b). The entire 35S-SS_{Tp}-MnSOD cassette was then isolated as a *BglII*–*BamHI* fragment and inserted into the dephosphorylated *BamHI* site of binary vector pGSC1702, yielding pChlSOD.

Downstream from the MnSOD sequences within pMitSOD and pChlSOD are the polyadenylation signals from the T-DNA-encoded gene 7 (Dhaese *et al.*, 1983) which are in addition to the endogenous MnSOD 3' sequences also present in each construct.

Transformation and propagation of plant material

Constructions were mobilized to *Agrobacterium tumefaciens* by 'ménage à trois' and the resulting strains were used to transform *N. tabacum* cv. PBD6 by leaf disc transformation (De Block *et al.*, 1987). Cuttings taken from regenerated plants were transferred to soil and grown under standard greenhouse conditions. Primary transformants were maintained and multiplied vegetatively.

Protein analysis, subcellular fractionations and immunogold labelling

Soluble proteins were extracted from plant material and assayed for SOD activity on native 10% polyacrylamide gels using the *in situ* staining technique of Beauchamp and Fridovich (1971) as previously described (Van Camp *et al.*, 1990). For subcellular fractionation, leaf material (20 g) was homogenized in 80 ml ice-cold homogenization buffer [50 mM Tris–HCl, pH 8.0, 0.33 M sucrose, 0.05% β -mercaptoethanol, 0.1% bovine serum albumin (BSA)], using a Waring blender (three low-speed pulses, 3 s each). After filtration through two layers of Miracloth[®], the homogenate was centrifuged in an SS34 rotor at 6000 r.p.m. for 30 s; chloroplasts were then prepared from the pellet on two-step Percoll gradients essentially as described (Mullet and Chua, 1983). A crude mitochondrial pellet was obtained from the supernatant of the initial low-speed centrifugation by an additional centrifugation at 15 000 r.p.m. for 12 min in an SS34 rotor. The pellet was resuspended in 2 ml suspension buffer (50 mM HEPES–KOH, pH 8.0, 0.33 M sorbitol, 0.1% BSA) and loaded onto two-step Percoll gradients as previously described (Bowler *et al.*, 1989a). The mitochondrial fraction was removed from the interface and was diluted 10-fold in suspension buffer. Both chloroplasts and mitochondria were pelleted by centrifugation

as before and were washed once more in suspension buffer. They were then resuspended in lysis buffer (25 mM Tris-HCl, pH 7.5, 0.5% β -mercaptoethanol) and insoluble material was removed by a further centrifugation step (13 000 r.p.m. for 12 min). All manipulations were carried out at 4°C.

Immunogold labelling of sections derived from leaves of control and transgenic plants were performed using polyclonal antibodies raised in rabbits against recombinant *N.plumbaginifolia* MnSOD purified from yeast (Bowler *et al.*, 1989b) and following the procedures described in De Clercq *et al.* (1990).

RNA analysis

Total RNA was prepared from fresh tissue as described by Jones *et al.* (1985) and quantified spectrophotometrically. For Northern analysis, 12 μ g was denatured in formaldehyde, electrophoresed and transferred to nylon membranes according to the manufacturer's recommendations (Amersham, Bucks, UK). To obtain a highly specific probe, the internal *HpaI*-*HindIII* fragment from pSOD1 (Bowler *et al.*, 1989a) was recloned in the *SmaI*-*HindIII* sites of pGem2 and ³²P-labeled single-stranded riboprobes were synthesized using T7 RNA polymerase (Promega). Northern hybridizations were performed as described (Bowler *et al.*, 1989a).

Methyl viologen treatment

Rectangular leaf discs of equal size (0.7 × 2.2 cm) were cut with a new surgical blade from leaves of soil-grown plants and floated on 0.4 M sorbitol. Each was then weighed and floated individually, top side up, on 3 ml water and methyl viologen (MV) solutions in 35 mm Petri dishes.

For light experiments leaf discs were first incubated in the dark for 16 h at room temperature ($\pm 23^\circ\text{C}$) to allow diffusion of the MV into the leaf, after which they were placed under a white light source for 2 hours (at 40 cm distance from two 20 W cool-white fluorescent tubes; light intensity 2.7 W/m²). Thereafter 20 μ M 3-(3,4-dichlorophenyl)-1,1'-dimethyl urea (DCMU) was added (final ethanol concentration 0.1% by volume) and the leaf discs were returned to the dark for 16 hours at 30°C. Ion leakage occurred in the course of this second dark incubation and was accelerated by the elevated temperature. DCMU was added in order to inhibit the reoxidation of QA, the first stable electron acceptor within the reaction center of photosystem II (Velthuys, 1981; Pfister *et al.*, 1981; Oettmeier and Soll, 1983). This was necessary for the fluorescence measurements and had no effect on ion leakage. In dark controls containing MV (which were given the same treatment except that they were not illuminated) no damage was observed by any of the criteria used, showing that all damage in these experiments was light mediated.

For dark experiments, leaf discs were incubated in complete darkness for 68 h at 30°C. This extended period and elevated temperature was necessary to generate sufficient quantifiable damage. DCMU was added after 54 h of dark incubation.

As mentioned in the text, three sets of control, MitSOD, and ChlSOD plants were tested during the course of these experiments. Although the results given are for only one of these sets, they are highly representative of the results obtained for each series. Nonetheless, the sensitivity of the leaf discs varied with age (the older the material the more resistant) and season (the higher the light intensity the more resistant) so it was necessary each time to determine the optimal non-saturating MV concentrations to use in order to reveal the differences. This lay between 0.5 and 3 μ M for our experimental conditions.

Conductance and fluorescence measurements

The solution on which the leaf discs had been floating was collected, made up to 3 ml (to correct for evaporation) and conductance was measured using KCl as a standard. The contribution of MV alone to the conductance was corrected for (this amounted to <5% of the reported values) and conductances were calculated per 35 mg fresh weight.

For fluorescence measurements, leaf discs were transferred to Petri dishes containing water plus 5 μ M DCMU and allowed to preadapt at room temperature in the dark for at least 1 h. Fluorescence of the leaf discs was excited by a broad band (400–650 nm) of blue light, and measured at wavelengths above 690 nm. The excitation light was switched on and off by means of an electronic shutter which opened within 2.5 ms. The output of the photomultiplier was fed into a storage oscilloscope (Nicolet Explorer IIIA) and then plotted on an X–Y plotter. Two measurements were made for each disc. For the first, the excitation light intensity was reduced 22-fold by means of a perforated aluminium disc, and the photomultiplier output was amplified by the same factor (by adjustment of the photomultiplier voltage). This allowed us to measure F_0 , the 'dark' fluorescence level. For the second measurement, we used the full light intensity (40 W/m²) with no amplification of the signal output. This allowed us to measure F_{\max} ,

the maximum fluorescence level. Φ II was calculated as $(F_{\max} - F_0)/F_{\max}$ (Genty *et al.*, 1989).

In some experiments we used a pulse-amplitude modulated fluorimeter (PAM101, Walz, Effeltrich, FRG) as described (Schreiber *et al.*, 1986), using leaf discs without DCMU. The results obtained with this apparatus were the same as those obtained with the above described method.

Phaeophytin measurements

Pigment extracts were prepared in chloroform:methanol essentially according to Bligh and Dyer (1959) and the absorbance spectra of the extracts were measured using a Cary spectrophotometer (Model 2300). The percentage of pheophytinized chlorophyll was calculated from the ratio $\Delta E_{538}/E_{665}$, where ΔE_{538} is the absorbance at 538 nm relative to a straight line connecting the two adjacent minima (at ~525 and 553 nm) and E_{665} is the absorbance at 665 nm (for chlorophyll, ΔE_{538} is zero). This calculation was based upon a calibration experiment in which all the chlorophyll in a pigment extract from untreated leaf discs (prepared as described above) was converted to pheophytin, and absorbance spectra were taken before and after pheophytinization (Slooten, L., Bowler, C., Vandenbranden, S., Van Montagu, M., Inzé, D. and Sybesma, C., in preparation).

Acknowledgements

We are greatly indebted to Allan Caplan, Arlette Reynaerts, Pamela Dunsmuir and Barry Halliwell for their constructive advice on our experiments, ideas and final manuscript. We thank Martine De Cock, Vera Vermaercke, Stefaan Van Gijsegem and Karel Spruyt for their invaluable help for the preparation of this manuscript, Paul Holvoet for the MnSOD antiserum, and Hilde Van de Wiele and Chris Genetello for plant transformation. This work was supported by grants from the International Atomic Energy Agency (no. 5285), the Services of the Prime Minister (UIAP 120CO187), and the 'ASLK-Kankerfonds' to M.V.M., and 'Fonds voor Geneeskundig Wetenschappelijk Onderzoek' (FGWO 33.0104.90) to M.V.M. and C.S. C.B. is supported by an SERC (NATO) Predoctoral Overseas Fellowship; L.S. is supported by the FGWO (grant no. 29.0221.0530) and D.I. is a Research Director of the Institut National de la Recherche Scientifique (France).

References

- Asada, K. and Takahashi, M. (1987) In Kyle, D.J., Osmond, C.B. and Arntzen, C.J. (eds), *Photoinhibition*. Elsevier Science Publishers B.V., Amsterdam, pp. 227–287.
- Avraham, K.B., Schickler, M., Sapoznikov, D., Yarom, R. and Groner, Y. (1988) *Cell*, **54**, 823–829.
- Bannister, J.V., Bannister, W.H. and Rotilio, G. (1987) *CRC Crit. Rev. Biochem.*, **22**, 111–180.
- Beauchamp, C.O. and Fridovich, I. (1971) *Anal. Biochem.*, **44**, 276–287.
- Biliński, T., Krawiec, Z., Liczmański, A. and Litwińska, J. (1985) *Biochem. Biophys. Res. Commun.*, **130**, 533–539.
- Bligh, E.G. and Dyer, W.J. (1959) *Can. J. Biochem. Physiol.*, **37**, 911–917.
- Bloch, C.A. and Ausubel, F.M. (1986) *J. Bacteriol.*, **168**, 795–798.
- Bowler, C., Alliotte, T., De Loose, M., Van Montagu, M. and Inzé, D. (1989a) *EMBO J.*, **8**, 31–38.
- Bowler, C., Alliotte, T., Van den Bulcke, M., Bauw, G., Vandekerckhove, J., Van Montagu, M. and Inzé, D. (1989b) *Proc. Natl. Acad. Sci. USA*, **86**, 3237–3241.
- Cadenas, E. (1989) *Annu. Rev. Biochem.*, **58**, 79–110.
- Carlioz, A. and Touati, D. (1986) *EMBO J.*, **5**, 623–630.
- Cashmore, A.R. (1983) In Kosuge, T., Meredith, C.P. and Hollaender, A. (eds) *Genetic Engineering of Plants. An Agricultural Perspective*. Plenum Press, New York, pp. 29–38.
- Chia, L.S., Mayfield, C.I. and Thompson, J.E. (1984) *Plant Cell Environ.*, **7**, 333–338.
- Clare, D.A., Rabinowitch, H.D. and Fridovich, I. (1984) *Arch. Biochem. Biophys.*, **231**, 158–163.
- Cornelissen, M. and Vandewiele, M. (1989) *Nucleic Acids Res.*, **17**, 19–29.
- Deblaere, R., Reynaerts, A., Höfte, H., Hernalsteens, J.-P., Leemans, J. and Van Montagu, M. (1987) *Methods Enzymol.*, **153**, 277–292.
- De Block, M., Botterman, J., Vandewiele, M., Dockx, J., Thoen, C., Gosselé, V., Movva, R., Thompson, C., Van Montagu, M. and Leemans, J. (1987) *EMBO J.*, **6**, 2513–2518.
- De Block, M., De Brouwer, D. and Tenning, P. (1989) *Plant Physiol.*, **91**, 694–701.
- De Clercq, A., Vandewiele, M., De Rycke, R., Van Damme, J., Van Montagu, M., Krebbers, E. and Vandekerckhove, J. (1990) *Plant Physiol.*, **92**, 899–907.

- Depicker, A., Stachel, S., Dhaese, P., Zambryski, P. and Goodman, H.M. (1982) *J. Mol. Appl. Genet.*, **1**, 561–573.
- Dhaese, P., De Greve, H., Gielen, J., Seurinck, J., Van Montagu, M. and Schell, J. (1983) *EMBO J.*, **2**, 419–426.
- Elroy-Stein, O. and Groner, Y. (1988) *Cell*, **52**, 259–267.
- Elroy-Stein, O., Bernstein, Y. and Groner, Y. (1986) *EMBO J.*, **5**, 615–622.
- Forman, H.J. and Boveris, A. (1982) In Pryor, W.A. (ed.), *Free Radicals in Biology*. Academic Press, New York, pp. 65–90.
- Foyer, C.H. and Halliwell, B. (1976) *Planta*, **133**, 21–25.
- Freeman, B.A. and Crapo, J.D. (1982) *Lab. Invest.*, **47**, 412–426.
- Garab, G., Lajkó, F., Mustárdy, L. and Márton, L. (1989) *Planta*, **179**, 349–358.
- Genty, B., Briantais, J.-M. and Baker, N.R. (1989) *Biochim. Biophys. Acta*, **990**, 87–92.
- Gruber, M.Y., Glick, B.R. and Thompson, J.E. (1990) *Proc. Natl. Acad. Sci. USA*, **87**, 2608–2612.
- Halliwell, B. (1984) *Chloroplast Metabolism—The Structure and Function of Chloroplasts in Green Leaf Cells*. Clarendon Press, Oxford.
- Halliwell, B. (1987) *FASEB J.*, **1**, 358–364.
- Harbour, J.R. and Bolton, J.R. (1975) *Biochem. Biophys. Res. Commun.*, **64**, 803–807.
- Imlay, J.A. and Linn, S. (1988) *Science*, **240**, 1302–1309.
- Jones, G.R.N. (1986) *Med. Hypothesis*, **21**, 267–271.
- Jones, J.D.G., Dunsmuir, P. and Bedbrook, J. (1985) *EMBO J.*, **4**, 2411–2418.
- Krause, G.H. (1988) *Physiol. Plant.*, **74**, 566–574.
- Krause, G.H. and Weis, E. (1984) *Photosynthesis Res.*, **5**, 139–157.
- Ksenzenko, M., Konstantinov, A.A., Khomutov, G.B., Tikhonov, A.N. and Ruuge, E.K. (1983) *FEBS Lett.*, **155**, 19–24.
- Law, M.Y., Charles, S.A. and Halliwell, B. (1983) *Biochem. J.*, **210**, 899–903.
- Lee, E.H. and Bennett, J.H. (1982) *Plant Physiol.*, **69**, 1444–1449.
- Mehler, A.H. (1951) *Arch. Biochem. Biophys.*, **33**, 65–77.
- Menzel, D.B. (1976) In Pryor, W.A. (ed.), *Free Radicals in Biology*. Academic Press, New York, Vol II, pp. 181–202.
- Monk, L.S., Fagerstedt, K.V. and Crawford, R.M.M. (1987) *Plant Physiol.*, **85**, 1016–1020.
- Mullet, J.E. and Chua, N.-H. (1983) *Methods Enzymol.*, **97**, 502–509.
- Nakano, Y. and Asada, K. (1980) *Plant Cell Physiol.*, **21**, 1295–1307.
- Oettmeier, W. and Soll, H.-J. (1983) *Biochem. Biophys. Acta*, **724**, 287–290.
- Orr, G.L. and Hogan, M.E. (1983) *Pestic. Biochem. Physiol.*, **20**, 311–319.
- Pfister, K., Steinback, K.E., Gardner, G. and Arntzen, C.J. (1981) *Proc. Natl. Acad. Sci. USA*, **78**, 981–985.
- Phillips, J.P., Campbell, S.D., Michaud, D., Charbonneau, M. and Hilliker, A.J. (1989) *Proc. Natl. Acad. Sci. USA*, **86**, 2761–2765.
- Rabinowitch, H.D., Sklan, D. and Budowski, P. (1982) *Physiol. Plant*, **54**, 369–374.
- Schreiber, U., Schliwa, U. and Bilger, W. (1986) *Photosynth. Res.*, **10**, 51–62.
- Shaaltiel, Y., Glazer, A., Bocion, P.F. and Gressel, J. (1988) *Pestic. Biochem. Physiol.*, **31**, 13–23.
- Siefermann-Harms, D. (1990) In Baltscheffsky, M. (ed.), *Current Research in Photosynthesis*. Kluwer, Dordrecht, Vol. II, pp. 245–248.
- Tanaka, K. and Sugahara, K. (1980) *Plant Cell Physiol.*, **21**, 601–611.
- Tanaka, K., Furasawa, I., Kondo, N. and Tanaka, K. (1988) *Plant Cell Physiol.*, **29**, 743–746.
- Tepperman, J.M. and Dunsmuir, P. (1990) *Plant Mol. Biol.*, **14**, 501–511.
- Van Camp, W., Bowler, C., Villarroel, R., Tsang, E.W.T., Van Montagu, M. and Inzé, D. (1990) *Proc. Natl. Acad. Sci. USA*, **87**, 9903–9907.
- van Loon, A.P.G.M., Pesold-Hurt, B. and Schatz, G. (1986) *Proc. Natl. Acad. Sci. USA*, **83**, 3820–3824.
- Velthuys, B.R. (1981) *FEBS Lett.*, **126**, 277–281.
- Welch, B.L. (1947) *Biometrika*, **34**, 28–35.
- Wong, G.H.W., Elwell, J.H., Oberley, L.W. and Goeddel, D.V. (1989) *Cell*, **58**, 923–931.

Received on February 1, 1991; revised on April 2, 1991